ISSN 1674-1056
http://cpb.iphy.ac.cn
http://iopscience.iop.org/cpb
中国物理 B
Chinese Physics
中国物理
Chinese Physics B

Nondestructive determination of film thickness with laser-induced surface acoustic waves

Xiao Xia(肖夏), Kong Tao(孔涛), Qi Hai Yang(戚海洋), Qing Hui Quan(秦慧全)

Citation: Chin. Phys. B . 2018, 27(9): 096802. **doi:** 10.1088/1674-1056/27/9/096802

Journal homepage: http://cpb.iphy.ac.cn; http://iopscience.iop.org/cpb

What follows is a list of articles you may be interested in

Influence of mode conversions in the skull on transcranial focused ultrasound and temperature fields utilizing the wave field separation method: A numerical study

Xiang-Da Wang(王祥达), Wei-Jun Lin(林伟军), Chang Su(苏畅), Xiu-Ming Wang(王秀明)

Chin. Phys. B . 2018, 27(2): 024302. **doi:** 10.1088/1674-1056/27/2/024302

Broadband acoustic focusing by symmetric Airy beams with phased arrays comprised of different numbers of cavity structures

Jiao Qian(钱姣), Bo-Yang Liu(刘博阳), Hong-Xiang Sun(孙宏祥), Shou-Qi Yuan(袁寿其), Xiao-Zhu Yu(俞笑竹)

Chin. Phys. B . 2017, 26(11): 114304. **doi:** 10.1088/1674-1056/26/11/114304

Theoretical analysis of interaction between a particle and an oscillating bubble driven by ultrasound waves in liquid

Yao-Rong Wu(武耀蓉), Cheng-Hui Wang(王成会)

Chin. Phys. B . 2017, 26(11): 114303. **doi:** 10.1088/1674-1056/26/11/114303

Wideband dispersion removal and mode separation of Lamb waves based on two-component laser interferometer measurement

Yan-Feng Xu(徐琰锋), Wen-Xiang Hu(胡文祥)

Chin. Phys. B . 2017, 26(9): 094301. **doi:** 10.1088/1674-1056/26/9/094301

Fabrication of VO_2 thin film by rapid thermal annealing in oxygen atmosphere and its metal-insulator phase transition properties

Liang Ji-Ran, Wu Mai-Jun, Hu Ming, Liu Jian, Zhu Nai-Wei, Xia Xiao-Xu, Chen Hong-Da

Chin. Phys. B . 2014, 23(7): 076801. **doi:** 10.1088/1674-1056/23/7/076801

Nondestructive determination of film thickness with laser-induced surface acoustic waves*

Xia Xiao(肖夏)†, Tao Kong(孔涛), Hai Yang Qi(戚海洋), and Hui Quan Qing(秦慧全)

School of Microelectronic, Tianjin Key Laboratory of Imaging and Sensing Microelectronic Technology, Tianjin University, Tianjin 300072, *China*

(Received 26 April 2018; revised manuscript received 24 June 2018; published online 28 August 2018)

The application of surface acoustic waves (SAWs) for thickness measurement is presented. By studying the impact of film thickness h on the dispersion phenomenon of surface acoustic waves, a method for thickness determination based on theoretical dispersion curve $v(fh)$ and experimental dispersion curve $v(f)$ is developed. The method provides a series of thickness values at different frequencies f, and the mean value is considered as the final result of the measurement. The thicknesses of six interconnect films are determined by SAWs, and the results are compared with the manufacturer's data. The relative differences are in the range from 0.4% to 2.18%, which indicates that the surface acoustic wave technique is reliable and accurate in the nondestructive thickness determination for films. This method can be generally used for fast and direct determination of film thickness.

Keywords: thickness measurement, dispersion curve, surface acoustic waves, layered structure

PACS: 68.55.jd, 43.35.+d, 61.05.–a **DOI:** 10.1088/1674-1056/27/9/096802

1. Introduction

Films are widely applied in aerospace, automotive manufacturing, biomedical engineering, and microelectronic industries.[1–4] In all such fields, the film thickness is one of the most important parameters for film quality evaluation. Yadav studied the influence of film thickness on structural, optical, and electrical properties of spray deposited antimony doped SnO_2 thin films.[5] Ren *et al.* studied the influence of thickness upon the interfacial water at the solid-liquid interface.[6] Yang *et al.* analyzed the influence of nanofilm thickness on the elastic properties of B2-NiAl.[7] So the film thickness is not only a parameter that characterizes the geometrical dimensions of the films, but also greatly affects the function and lifetime of the films. Therefore, film thickness determination is an important requirement in many fields of technology.

In order to keep the function of the films after thickness measurement, many nondestructive testing methods have been proposed to measure the film thickness, including eddy current, spectroscopic ellipsometry, and x-ray transmission.[8–15] These methods work well, but they are all restricted to certain types of materials. The eddy current method is more suitable to measure the thickness of the non-conductive coating on the non-magnetic metal substrate.[8–10] The spectroscopic ellipsometry is an optical method. The measured material should be transparent.[11–13] The x-ray transmission needs the absorption coefficients of the film and substrate to have obvious differences. The limitation for its wide application can be found when the chemical composition of the film is close to that of the substrate.[14,15]

Surface acoustic waves (SAWs) are dispersive during propagating on a layered structure, the surface acoustic waves with different frequencies have different propagation velocities. Due to this feature, the surface acoustic wave method can be applied to film thickness determination. This method is fast, simple, and non-destructive.[16–18] In addition, the propagation of SAWs is hardly limited by the material. So this method is suitable to determine the film thicknesses of most materials.

In this paper, the relationship between the geometrical parameter thickness and the dispersion phenomenon of surface acoustic waves is analyzed. Accordingly, a thickness calculation method is developed by using the theoretical dispersion curve $v(fh)$. The thickness calculation of two standard SiO_2 films with this method is described in detail. In addition, four low dielectric constant (low-k) samples are also investigated in this study. The results of the six samples are compared with the manufacturer's data. Comparing the results shows that the thicknesses of the interconnect films can be sensitively detected by the SAWs measurement.

2. Theoretical background

Surface acoustic waves propagate along the surface of a material. The penetration depth of the wave is defined to be equal to the wavelength λ and it reduces with increasing frequency.[16] In a homogeneous and isotropic bulk material, the wave phase velocity v depends on the material parameters: Young's modulus E, density ρ, and Poisson's ratio σ, and it is independent of the frequency f of the wave.[19,20]

*Project supported by the National Natural Science Foundation of China (Grant No. 61571319).

†Corresponding author. E-mail: xiaxiao@tju.edu.cn

© 2018 Chinese Physical Society and IOP Publishing Ltd

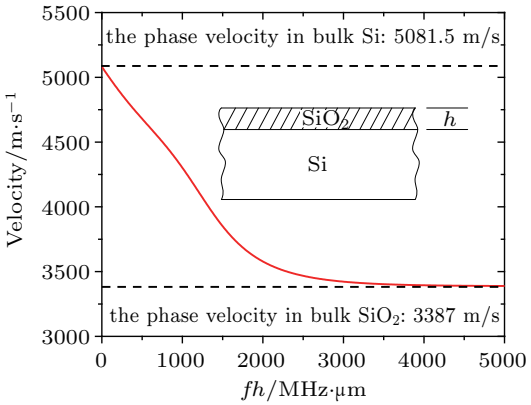


Fig. 1. (color online) The theoretical dispersion curve $v(fh)$ of SiO_2/Si structure.

In the film/substrate structure, the phase velocity v of the waves depends on the film and substrate material parameters and the frequency–thickness product fh.[21,22] The surface acoustic waves are dispersive, and the dispersion phenomenon is resulted from the different SAW phase velocities in the film and substrate materials. Figure 1 illustrates the dispersion phenomenon, it shows the theoretical dispersion curve $v(fh)$ of the SiO_2/Si structure. The SAWs propagate along the [110] direction of the silicon. The phase velocities of SAWs in bulk Si and bulk SiO_2 are 5081.5 m/s and 3387 m/s, respectively. Because the penetration depth of the wave reduces with the increase of the frequency, lower frequency waves are more affected by the Si substrate. So their propagation velocities are closer to those in bulk Si. In contrast, higher frequency waves are more influenced by the SiO_2 film, and their propagation velocities are closer to those in bulk SiO_2.

In addition to the frequency, the film thickness has the same effect on the phase velocity of SAWs. The increase of the film thickness can expand the influence of the SiO_2 film on SAWs propagation. So the increases of the frequency and the film thickness together result in the change of the wave velocity. According to the physical principles of the elastodynamic theory, the phase velocity v of the waves is a function of the frequency–thickness product fh on the condition that the material parameters of the film and substrate are determinate.

For the thickness determination, the SAWs experiment can provide the v (f) curve of the sample. This curve contains information about the film thickness. With the material parameters of the sample, the relationship between the phase velocity v and the frequency–thickness product fh can be calculated. By using the theoretical dispersion curve $v(fh)$ and experimental dispersion curve $v(f)$, the film thickness can be obtained.

3. Experimental procedure

Figure 2 shows the schematic of a surface acoustic wave experimental system. A pulsed laser with a 0.8 ns pulse in width and 337.1 nm in wavelength is used to generate wideband surface acoustic waves in the test. A cylindrical lens makes the laser beam focus into a line source on the surface of the sample. The surface acoustic waves propagate along the sample and are detected by a piezoelectric detector. A polyvinyllidene fluoride (PVDF) foil is pressed by the wedge-shape knife edge of the detector. It is used to transfer the broad range of vibration signals into electric signals. The electric signals are amplified by an amplifier and recorded by a digital oscilloscope.

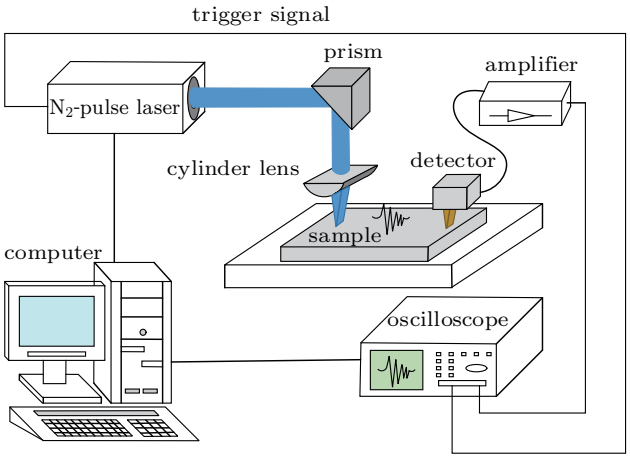


Fig. 2. (color online) Schematic of laser-induced surface acoustic wave experimental system.

Two standard SiO_2 films with different thicknesses are firstly tested by the SAWs technique to check our method. These films are grown by thermal oxidation on Si substrate. The material parameters of the standard SiO_2 film include Young's modulus $E = 72$ GPa, density $\rho = 2.2$ g/cm^3, and Poisson's ratio $\sigma = 0.17$. Surface acoustic waves are generated on the sample surface and arranged to propagate in the [110] direction of silicon.

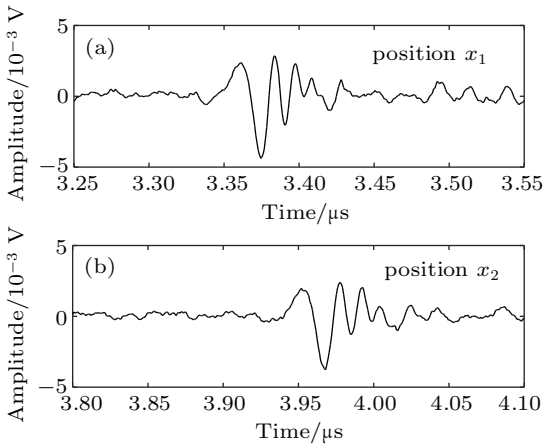


Fig. 3. The SAWs signals detected at different distances (a) x_1 and (b) x_2 away from the line-shaped laser source on SiO_2 I.

In order to obtain the experimental dispersion curve, the electric signals $u_i(t)$ (i indicates different laser position) are detected at two different distances x_1 and x_2 away from the

line-shaped laser source. The SAWs signals of SiO_2 I detected at two different positions are shown in Fig 3. The distance between the two detection positions is 3 mm. The two signals have an apparent delay because of the different propagation distances. The electric signals $u_i(t)$ are handled by Fourier-transform to obtain the phase angles $\Phi_i(f)$.[23] The phase velocity $v(f)$ can be calculated by the following equation:

$$v(f) = \frac{2\pi f(x_2 - x_1)}{\Phi_2(f) - \Phi_1(f)}, \tag{1}$$

where $\Phi_1(f)$ and $\Phi_2(f)$ are the phase angles of the SAW signals detected at positions x_1 and x_2, respectively.

4. Determining the thickness

Figure 4 shows the dispersion curves obtained from the above experiments for the two SiO_2 samples. In order to reduce the vibration of the curves, two fitting curves of the experimental dispersion curves are calculated by polynomial fitting. The fitting equations of SiO_2 I and SiO_2 II respectively are

$$SiO_2\ \mathrm{I}: v = -0.45909 f_{\mathrm{exp}} + 5081.5, \tag{2}$$

$$SiO_2\ \mathrm{II}: v = -0.89884 f_{\mathrm{exp}} + 5081.5. \tag{3}$$

A method to determine the thickness is developed by combining the theoretical dispersion curve $v(fh)$ and experimental dispersion curve. Because the two SiO_2 films employed in this research have the same material parameters, the same theoretical dispersion curve $v(fh)$ is used to calculate the thicknesses of the films. Figure 5 shows this theoretical curve $v(fh)$, which is the initial part of the curve in Fig. 1. The details of this method are given as follows. Select one data point $(fh_{\mathrm{theoty}}, v)$ on the theoretical dispersion curve $v(fh)$. Take the velocity v of this data point into the fitting equation of the experimental dispersion curve, the related frequency f_{exp} can be calculated. It means the same value of velocity v correlates the theoretical dispersion curve $v(fh)$ and the experimental dispersion curve. At last, the thickness h can be easily obtained by comparing the frequency–thickness product fh_{theoty} of the theoretical dispersion curve and the frequency f_{exp} of the experimental dispersion curve,

$$h = \frac{fh_{\mathrm{theoty}}}{f_{\mathrm{exp}}}. \tag{4}$$

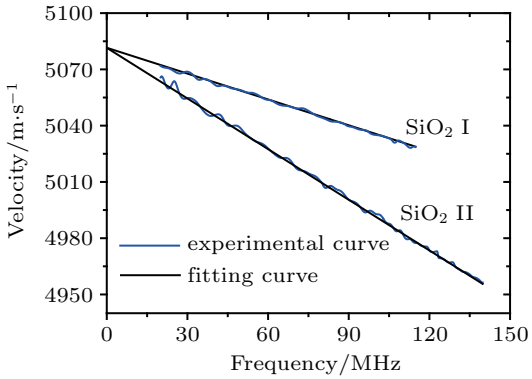


Fig. 4. Experimental dispersion curves and fitting curves of two SiO_2 samples.

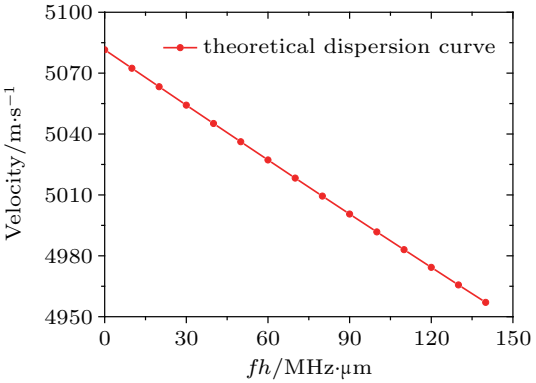


Fig. 5. (color online) The theoretical dispersion curve $v(fh)$ used to determine the thicknesses of SiO_2 films.

Table 1. The data of the theoretical curve, the frequencies f_{exp} of two experimental dispersion curves, and calculation results of the two SiO_2 films.

Theoretical curve		SiO_2 I		SiO_2 II	
fh_{theoty}/MHz·μm	v/m·s^{-1}	f_{exp}/MHz	h/nm	f_{exp}/MHz	h /nm
10	5072.4	19.8	504.4	–	–
20	5063.3	39.6	504.4	19.9	1004.1
30	5054.2	59.4	505.0	30.0	999.7
40	5045.2	79.1	505.7	40.1	998.4
50	5036.2	98.7	506.6	50.1	998.5
60	5027.2	118.2	507.5	60.0	999.2
70	5018.3	–	–	70.0	1000.3
80	5009.4	–	–	79.9	1001.7
90	5000.6	–	–	89.7	1003.4
100	4991.8	–	–	99.5	1005.2
110	4983.0	–	–	109.2	1007.1
120	4974.3	–	–	118.9	1009.2
130	4965.7	–	–	128.5	1011.3
140	4957.0	–	–	138.1	1013.6

Because theoretical dispersion curve $v(fh)$ contains many data points, a series of thickness values can be calculated from different data points. Table 1 shows the data of the theoretical curve $v(fh)$ in Fig. 5, the frequencies $f_{\rm exp}$ of the two experimental dispersion curves, and the calculation results of the two SiO_2 films. The frequencies $f_{\rm exp}$ of the experimental dispersion curves are solved by taking the values of velocity v into Eqs. (2) and (3), respectively. For SiO_2 I, because the frequency f of the experimental dispersion curve is in the range from 20 MHz to 120 MHz, six data with $f_{\rm exp} = 19.8$ MHz to 118.2 MHz are chosen to calculate the thickness. The six calculated results vary only a little, and the mean value 505 nm is considered as the final result. For SiO_2 II, the data with $f_{\rm exp} = 19.9$ MHz to 138.1 MHz are in the range of the experimental dispersion curve. The mean value of the calculated thicknesses is 1004 nm. The manufacturer's data of these two standard SiO_2 films are 500 ± 2 nm and 1000 ± 2 nm, respectively. So the thicknesses determined from the proposed SAWs method agree very well with the manufacturer's data. The relative differences between the SAWs results and manufacturer's data for the two films are only 1% and 0.4%, respectively.

5. Application of the method to low-k samples

Low dielectric constant (low-k) materials are very important to decrease the *RC* delay in interconnects of integrated circuits.[24,25] The combination of the low-k insulator with lower resistivity metal of Cu is widely used in high speed ultra large-scale integration devices.

The thicknesses of four low-k samples are measured by the proposed SAWs method in this study. Figure 6 shows the experimental dispersion curves and fitting curves of the four samples. These low-k samples are divided into two groups based on the materials of the films. Two films are made of porous black diamond (BD) material, and the other two films are composed of dense black diamond material. The material parameters are listed in Table 2, and they are used to calculate the related theoretical dispersion curves $v(fh)$.

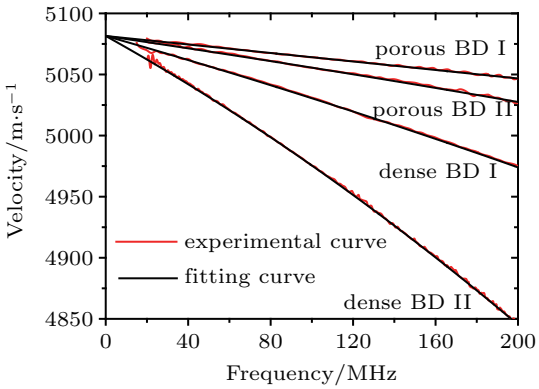


Fig. 6. (color online) Experimental dispersion curves and fitting curves of four low-k samples.

Table 2. Material parameters of porous and dense black diamond low-k samples.

Material	Young's modulus/GPa	Density/g·cm^{-3}	Poisson's ratio
Porous BD	1.34	1.1	0.18
Dense BD	9.5	1.38	0.18

The thicknesses of these samples determined by the SAWs method and the manufacturer's data are listed in Table 3. As shown in Table 3, there is a good agreement between the SAWs results and the manufacturer' s data, the largest relative difference between the two sets of data is only 2.18%, which occurs for the dense black diamond II.

Table 3. Summary of thicknesses obtained from the surface acoustic wave method and manufacturer's data.

Sample	SAW method/nm	Manufacturer's data/nm	Relative difference/%
Porous BD I	198	197 ± 5	0.50
Porous BD II	298	304 ± 7	2.00
Dense BD I	509	506 ± 10	0.58
Dense BD II	1006	1028 ± 20	2.18

6. Conclusion

The surface acoustic wave technique is applied to measure the thicknesses of films of ULSI. A thickness calculation method is developed based on the union of experimental dispersion curve and theoretical dispersion curve $v(fh)$. This calculation method is very simple and fast. A series of thickness values can be calculated at different frequencies f of the experimental dispersion curve. The mean value is considered as the final result of the measurement. So there is another advantage of the method that multiple thickness values can reduce the uncertainty of single data and increase the reliability of the measurement result. Six interconnect films are employed to verify our method. The results of these films are compared with the manufacturer's data. For these six films, the relative differences between the measurement results and manufacturer's data are only in the range from 0.4% to 2.18%. The remarkable agreement of the contrast results shows the potential and reliability of the surface acoustic wave technique.

References

[1] Fourez S, Jenot F, Ouaftouh M, Duquennoy M and Ourak M 2012 *Meas. Sci. Technol.* **23** 085608

[2] Dong G C, Baarle D V, Frenken J and Tang Q W 2016 *Chin. Phys. Lett.* **33** 116101
[3] Zalnezhad E and Sarhan A A D 2014 *Int. J. Adv. Manuf. Technol.* **72** 1491
[4] Gu S S, Hu X J and Huang K 2013 *Acta Phys. Sin.* **62** 118101 (in Chinese)
[5] Yadav Y Y 2015 *Thin Solid Films* **591** 18
[6] Ren X P, Zhou B, Li L T and Wang C L 2013 *Chin. Phys. B* **22** 016801
[7] Yang X Y, Zhang J P, Wu Y R and Liu F S 2015 *Acta Phys. Sin.* **64** 016803 (in Chinese)
[8] Yin W and Peyton A J 2007 *NDT E Int.* **40** 43
[9] Qu Z, Zhao Q and Meng Y 2014 *NDT E Int.* **61** 53
[10] Chen X L and Lei Y Z 2015 *Chin. Phys.* B **24** 030301
[11] Franquet A, Terryn H and Vereecken J 2003 *Thin Solid Films* **441** 76
[12] Gong J B, Dong W L, Dai R C, Wang Z P, Zhang Z M and Ding Z J 2014 *Chin. Phys. B* **23** 087802
[13] Zhao J M and Yang P 2012 *Microsyst. Technol.* **18** 1455
[14] Ying A J, Murray C E and Noyan I C 2009 *J. Appl. Crystallogr.* **42** 401
[15] Kolbe M, Beckhoff B, Krumrey M and Ulm G 2005 *Pectroc. Acta Pt. B-Atom. Spectr.* **60** 505
[16] Schneider D, Hofmann R, Schwarz T, Grosser T and Hensel E 2012 *Surf. Coat. Technol.* **206** 2079
[17] Xiao X, Qi H Y, Tao Y and Kikkawa T 2016 *Appl. Surf. Sci.* **388** 448
[18] Xiao X, Sun Y and Shan X M 2012 *Surf. Coat. Technol.* **207** 240
[19] Schneider D, Schulz S E and Gessner T 2005 *Microelectron. Eng.* **82** 393
[20] Xiao X, Qi H Y, Sui X L and Kikkawa T 2017 *Appl. Surf. Sci.* **399** 599
[21] Farnell G W and Adler E L 1972 *Phys. Acoust.* (Vol. 9) (New York: Academic) pp. 35–127
[22] Xiao X, Hata N, Yamada K and Kikkawa T 2004 *Jpn. J. Appl. Phys.* **43** 508
[23] Xiao X, Shan X M, Kayaba Y, Kohmura K, Tanaka H and Kikkawa T 2011 *Microelectron. Eng.* **88** 666
[24] Grill A, Gates S M, Ryan T E, Nguyen S V and Priyadarshini D 2014 *Appl. Phys. Rev.* **1** 011306
[25] Xiao X, Tao Y and Sun Y 2014 *Chin. Phys. B* **23** 106803